Inorganic Chemistry

Article

pubs.acs.org/IC

Homoleptic Transition Metal Complexes of the 7-Azaindolide Ligand Featuring κ^1-N1 Coordination

Jacob A. Przyojski,[§,†] Monica L. Kiewit,[§,†] Kathlyn L. Fillman,[†,‡] Hadi D. Arman,[†] and Zachary J. Tonzetich*[,†]

[†]Department of Chemistry, University of Texas at San Antonio (UTSA), San Antonio, Texas 78249, United States

[‡]Department of Chemistry, University of Rochester, Rochester, New York 14627, United States

Supporting Information

ABSTRACT: Homoleptic complexes of the anion of 7-azaindole (AzaIn) were synthesized and characterized for a series of 3d transition metals. For Mn(II), Fe(II), and Co(II), complexes of formula $Na_2[M(AzaIn)_4]\cdot 2L$ (L = tetrahydrofuran (THF), 2-MeTHF, toluene, or benzene) were isolated by treatment of the corresponding metal chloride salts with 7-azaindole in the presence of sodium hexamethyldisilazide. The complexes adopt tetrahedral geometries with exclusive coordination to the transition metal ion through the pyrrolic N1 nitrogen atoms of the AzaIn ligands. Solid-state structures of the complexes demonstrate that the sodium cations remain tightly associated with the coordination entities through interaction with both the pyrrolic and pyridine nitrogen atoms of the azaindolide ligands. For Fe(II), replacement of the sodium cations by other alkali metal ions (Li or K) generates new complexes that demonstrate similar coordination geometries to the sodium salts. As a means of comparison, the Fe(II) complex of 4-azaindolide was also investigated. $Na_2[Fe(4\text{-}AzaIn)_4]\cdot 2L$ adopts a similar solution structure to the 7-azaindolide complexes as judged by NMR spectroscopy and cyclic voltammetry. Density functional theory calculations were performed to investigate the bonding in the 7-azaindolide complexes. Results demonstrate that 7-azaindolide-κ^1-N1 is a nearly pure sigma donor ligand that features a high degree of ionic character in its bonding to mid 3d transition metal ions.

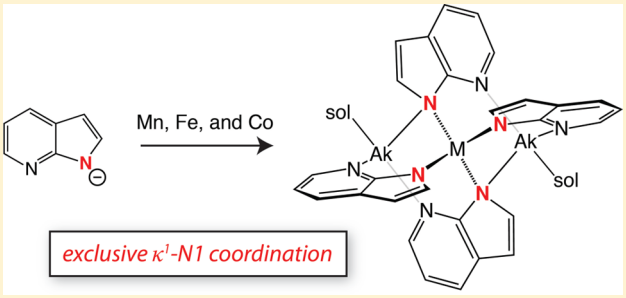

INTRODUCTION

Coordination of nitrogen heterocycles to transition metal ions remains an enduring theme in inorganic and bioinorganic chemistry. Of the multitude of different ligands composed of nitrogen heterocycles, those that feature pyridine and pyrrole units are among the most frequently encountered both individually and as components of chelates. The fusion of these two units gives rise to the azaindole family of molecules (Chart 1). This class of heterocycles has received significant attention because of the biological activity of certain derivatives and the structural relationship between azaindoles and the purine bases found in nucleic acids.[1−7] Despite this interest, only a limited body of work has investigated the coordination chemistry of these molecules with transition metals.

Chart 1. Azaindole Family of Molecules

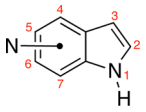

The most commonly encountered member of the azaindole family is 7-azaindole. In its neutral and deprotonated forms, 7-azaindole is capable of a wide variety of binding modes to metal ions through both nitrogen atoms N1 and N7 (Chart 2).[7] Coordination of the π face of the pyrrole moiety in an η^5-fashion has also been reported for a purported titanocene dichloride analogue, although no solid-state structure exists for this compound.[8] Of the transition metal complexes of 7-azaindole reported to date, the majority incorporate multiple metal centers in bridging or direct M−M bonding motifs.[9−17] For those complexes that contain only a single transition metal ion, coordination of the 7-azaindole primarily occurs through the pyridine N7 atom.[18−28] In very few instances have transition metal complexes featuring exclusive κ^1-N1 coordination been reported,[29−31] although this coordination mode is

Chart 2. Coordination Modes of 7-Azaindole

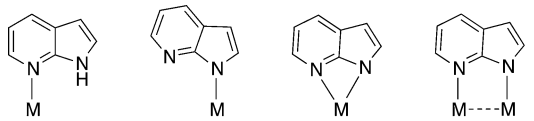

Received: July 30, 2015
Published: September 17, 2015

DOI: 10.1021/acs.inorgchem.5b01732
Inorg. Chem. 2015, 54, 9637−9645

better established for main group metals such as aluminum.[32−34] In addition to binding to metals in its neutral and deprotonated forms, the 7-azaindole moiety has also been incorporated into a variety of chelating ligands.[35−37] In such complexes, coordination is again primarily observed through the N7 atom.[38−42]

Given the dearth of complexes that demonstrate coordination through the pyrrolic nitrogen, and the straightforward parallels to pyrrolide and indolide complexes, we became interested in the chemistry of 7-azaindole complexes that display coordination through the N1 atom. We report here our findings concerning the synthesis and electronic structure of homoleptic complexes of the first row transition metals featuring this binding mode. We also report the synthesis of the first example of a homoleptic 4-azaindole complex, which displays similarities to the 7-azaindole compounds.

RESULTS AND DISCUSSION

Synthesis of 7-Azaindolide Complexes. Reaction in tetrahydrofuran (THF) of 4 equiv of 7-azaindole (HAzaIn) with MCl_2 (M = Mn, Fe, or Co) in the presence of 4 equiv of NaHMDS (HMDS = hexamethyldisilazide) produced the homoleptic 7-azaindolide complexes, $Na_2[M(AzaIn)_4]\cdot 2THF$ (eq 1: M = Mn, **1·thf**; Fe, **2·thf**; and Co, **3·thf**). The

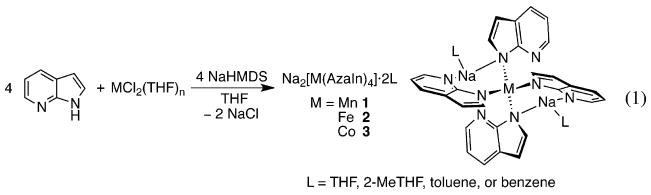

(1)

compounds are soluble in arene solvents and retain 2 equiv of THF as judged by ^{1}H NMR spectroscopy. Each of the compounds can be conveniently recrystallized from 2-MeTHF/pentane solutions affording the corresponding 2-MeTHF solvates (**1−3·mthf**). Solution magnetic susceptibility measurements for **1−3·mthf** are consistent with high-spin M^{2+} ions, with each complex displaying several broadened NMR signals for the coordinated azaindolide ligands in benzene-d_6 (see Supporting Information). In addition, peaks due to the associated 2-MeTHF molecules are readily apparent. The 2-MeTHF peaks in all three complexes are broadened and shifted from their values in the free molecule indicating that some degree of interaction persists in benzene solution (vide infra). Each complex is very sensitive to the ambient atmosphere, decomposing in a matter of seconds (M = Mn, Fe) to minutes (M = Co) upon exposure to air in both the solid state and solution.

Crystals of complexes **1−3** suitable for X-ray diffraction were obtained by vapor diffusion of pentane into saturated solutions of THF, toluene, or benzene. The resulting solid-state structures for all complexes are quite similar, differing only in the nature of the solvent molecules coordinated to the associated sodium cations. Two representative structures, those of **3·thf** and **3·tol**, are depicted in Figure 1. Structures of **1·tol**, **2·thf**, and **2·benz** were also obtained and appear in the Supporting Information.

In the solid state, complexes **1−3** feature tetrahedral coordination geometries about the transition metal ions with exclusive coordination through the pyrrolide nitrogen atoms, N1. The charge on each coordination entity is balanced by two sodium cations, which associate tightly with each complex explaining the observed solubility in arene solvents. The coordination sphere of the sodium cations comprises the pyridine nitrogen atoms (N7) of each azaindolide ligand, the pyrrolide moieties of two of the four azaindolide ligands, and a solvent molecule. Interaction of the sodium cations with the pyrrolide groups most likely attenuates the basicity of the azaindolide ligand. Similar behavior has been observed previously with homoleptic naphthalide and alkoxide complexes of the mid 3d metals.[43−50] In the case of the benzene adduct of **2** (**2·benz**), the complex crystallizes as a coordination polymer featuring sodium coordination to the C2−C3 π-bond of an adjacent azaindolide ligand in place of one Na-benzene interaction (see Supporting Information). In all cases, the bond metrics about the metal centers are consistent with high-spin ions corroborating solution magnetic susceptibility measurements.

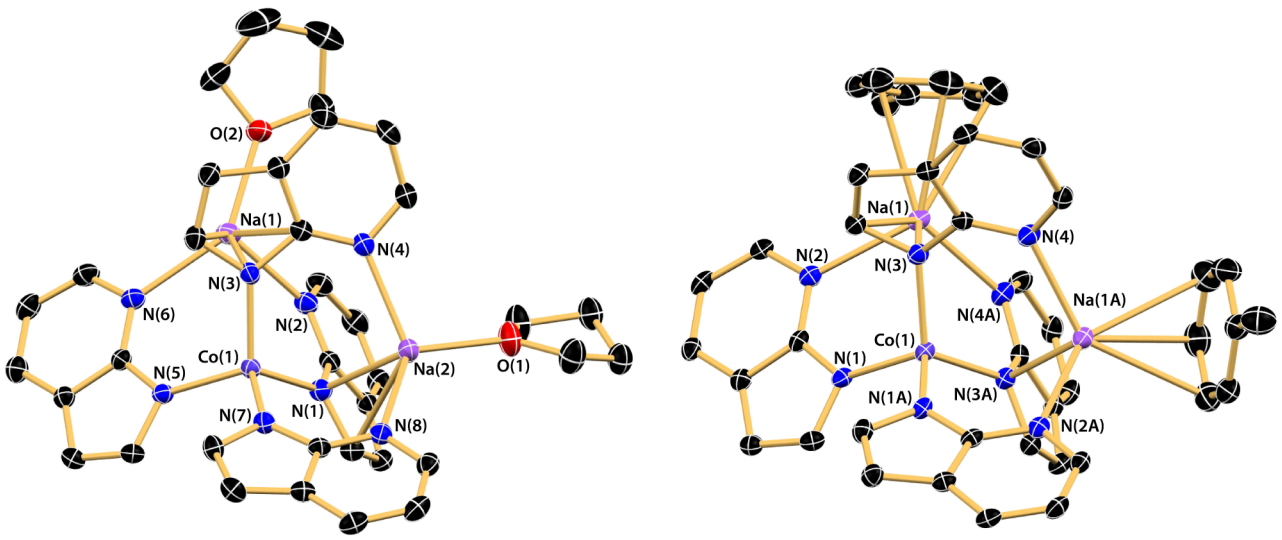

Figure 1. Thermal ellipsoid drawings (50%) of **3·thf** and **3·tol**. Hydrogen atoms are omitted for clarity. Selected average bond distances and angles for compounds **1−3** can be found in Table 1.

DOI: 10.1021/acs.inorgchem.5b01732
Inorg. Chem. 2015, 54, 9637−9645

The solution behavior of **2·mthf** and **3·mthf** was next scrutinized by ^{1}H NMR spectroscopy to compare the nature of the sodium cation interactions with that observed in the solid state. The Mn congener, **1**, was not examined in detail because it displays a nearly featureless NMR spectrum. For both **2·mthf** and **3·mthf**, four paramagnetically shifted azaindole resonances are observable between −10 and +35 ppm in benzene-d_6. Integration of these peaks versus those of 2-MeTHF demonstrates that each corresponds to four hydrogen atoms. Thus, all four azaindolide ligands appear to be equivalent on the NMR time scale. This situation does not reflect the solid-state structure of the complexes, which feature two different azaindolide environments by virtue of tight sodium cation association (vide supra). The apparent equivalency of the four azaindolide ligands must therefore result from fluxional behavior of the sodium cations on the NMR time scale. Dissociation of the sodium cations in benzene is unlikely given the solubility of the complexes and the observed broadening and shifting of the 2-MeTHF resonances. In contrast to benzene-d_6, spectra of both **2·mthf** and **3·mthf** in the more-coordinating solvent, acetonitrile-d_3, display resonances for free 2-MeTHF indicating that the ether does not interact with the complexes upon dissolution in this solvent. Moreover, each of the azaindole resonances becomes sharper in acetonitrile-d_3, especially those of **3**, and a fifth azaindole resonance becomes visible as a broadened peak downfield of +60 ppm (see Supporting Information).

Spectra of **2** and **3** in acetonitrile suggest that the sodium cations might dissociate from the azaindolide ligands to a significant degree in sufficiently polar solvents. To examine this possibility further, the cobalt complex **3·mthf** was treated with the cryptand molecule, Kryptofix 222. Addition of 1 and 2 equiv of Kryptofix 222 to **3·mthf** in acetonitrile-d_3 resulted in changes to the ^{1}H NMR spectrum consistent with encapsulation of the sodium cations by the cryptand molecule (see Supporting Information). Furthermore, addition of 2 equiv of Kryptofix to a toluene solution of **3·mthf** resulted in immediate precipitation of a blue solid (eq 2). The blue solid

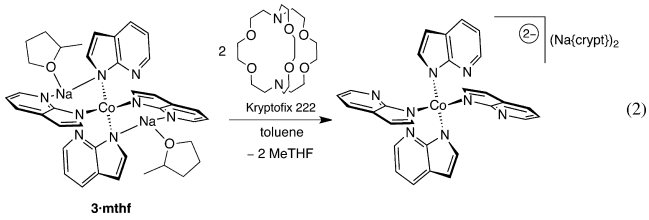

(2)

demonstrated no solubility in toluene or THF, dissolving only in CH_2Cl_2 and acetonitrile. Such solubility is consistent with a doubly charged salt of the form $(Na\{crypt\})_2[Co(AzaIn)_4]$. Unfortunately, attempts to crystallize the blue solid for purification and further analysis were unsuccessful.

The synthesis of the iron complex, $[Fe(AzaIn)_4]^{2-}$, was also investigated using both KHMDS and LiHMDS as bases. In similar fashion to the reaction in eq 1, reaction of $FeCl_2(THF)_{1.5}$ with 7-azaindole in the presence of KHMDS afforded a homoleptic azaindolide complex (**4**, eq 3). In

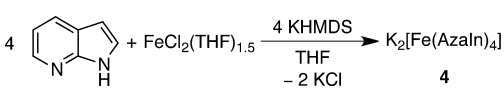

(3)

contrast to **2**, complex **4** was found to be insoluble in benzene and toluene. The complex did dissolve readily in coordinating solvents such as THF and acetonitrile. ^{1}H NMR spectra of **4** in acetonitrile-d_3 were very similar to those of **2·mthf** in the same solvent, displaying five paramagnetically shifted azaindole resonances between −10 and +75 ppm. Unlike **2**, however, spectra of **4** did not demonstrate evidence for solvent incorporation suggesting that the complex exists as a solvent-free species in the solid state.

Crystallization of **4** from benzene in the presence of THF produced crystals suitable for X-ray diffraction. Figure 2 depicts

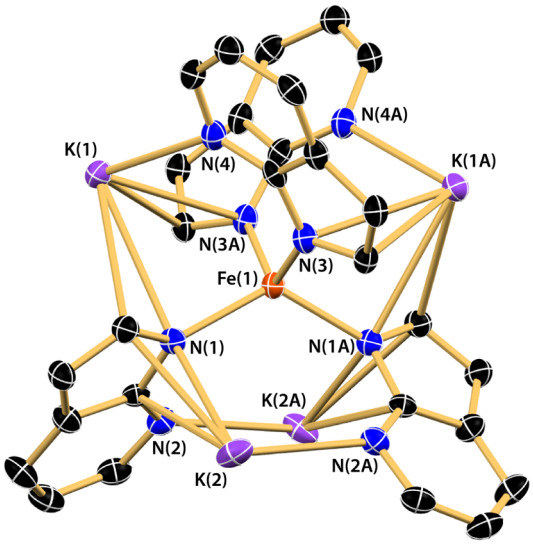

Figure 2. Thermal ellipsoid rendering (50%) of the solid-state structure of $K_2[Fe(AzaIn)_4]$, **4**. The solid-state network is truncated to display a single coordination entity. Hydrogen atoms are omitted for clarity. Selected bond distances (Å) and angles (deg): Fe(1)−N(1) = 2.056(2); Fe(1)−N(3) = 2.047(2); Fe(1)−K(1) = 3.6249(11); Fe(1)−K(2) = 3.8683(10); K(1)−N(4) = 2.785(3); K(2)−N(2A) = 2.819(3); N(1)−Fe(1)−N(1A) = 122.40(13); N(3)−Fe(1)−N(3A) = 122.04(14); N(1)−Fe(1)−N(3) = 103.45(9); N(1A)−Fe(1)−N(3) = 103.54(10).

the solid-state structure of **4**. Unlike the sodium salts, complex **4** forms a coordination network in the solid state explaining its observed insolubility in arene solvents. The iron ion in **4** displays an axial distortion from ideal tetrahedral geometry but remains coordinated by four N1 atoms of the azaindolide ligands. There are two types of potassium cations in the asymmetric unit. One type displays coordination to a single N7 pyridine atom, whereas the other displays coordination to two different N7 pyridine atoms. The remaining coordination sphere for each type of potassium cation is completed by interactions with the π faces of multiple pyrrolide moieties (Figure 2). Despite the differences in solid-state structure, the average bond lengths from iron to the pyrrolic nitrogen atoms in **4** are only slightly elongated from those of **2·thf** (cf. 2.051(2) Å vs 2.042(2) Å).

In similar fashion to Na- and KHMDS, reactions of LiHMDS with $FeCl_2(THF)_{1.5}$ and 7-azaindole afforded a homoleptic azaindolide complex (eq 4, **5·thf**). Isolation of **5·thf** proved

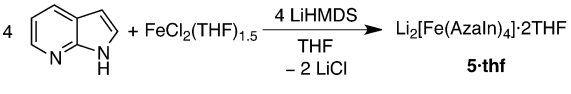

(4)

somewhat more difficult than **2·thf** and **4**, requiring optimization of the synthetic procedure. Unlike **2·thf** and **4**,

DOI: 10.1021/acs.inorgchem.5b01732
Inorg. Chem. 2015, 54, 9637−9645

5·thf is only sparingly soluble in THF, yet it dissolves in arene solvents. ^{1}H NMR spectra of **5·thf** in benzene-d_6 display two sets of inequivalent azaindole resonances suggesting that the Li cations are not fluxional on the NMR time scale at room temperature. However, use of acetonitrile-d_3 in place of benzene-d_6 as an NMR solvent did result in a spectrum for **5** much more similar to those of **2** and **4** (see Supporting Information). This observation suggests that the solution structures of **2**, **4**, and **5** are nearly identical in polar solvents such as acetonitrile.

Further confirmation for the structure of **5·thf** was provided by X-ray crystallography. The solid-state structure is depicted in Figure 3 and is very similar to that of **2·thf**. The average bond

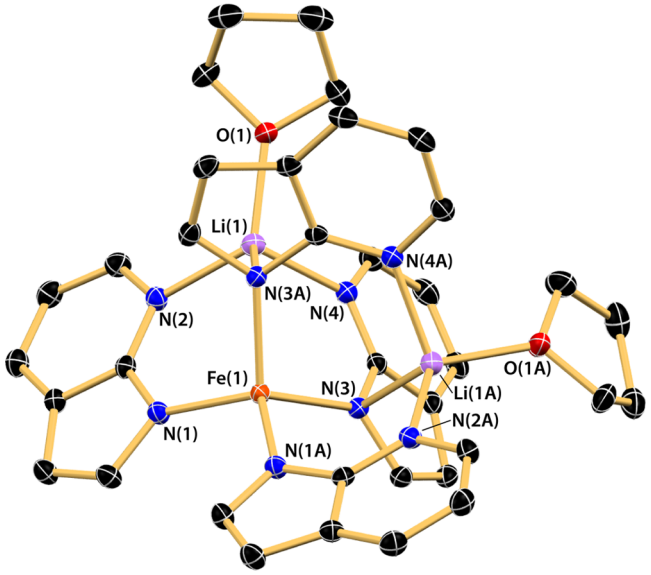

Figure 3. Thermal ellipsoid rendering (50%) of the solid-state structure of $Li_2[Fe(AzaIn)_4]\cdot 2THF\cdot C_6H_6$, **5·thf**. Hydrogen atoms and cocrystallized benzene molecule are omitted for clarity. Selected bond distances (Å) and angles (deg): Fe(1)–N(1) = 2.0175(11); Fe(1)–N(3) = 2.0674(11); Fe(1)–Li(1) = 3.021(2); Li(1)–N(2) = 2.034(2); Li(1)–N(4) = 2.015(2); Li(1)–N(3A) = 2.234(2); N(1)–Fe(1)–N(1A) = 112.48(6); N(3)–Fe(1)–N(3A) = 106.91(6); N(1)–Fe(1)–N(3) = 114.03(4); N(1)–Fe(1)–N(3A) = 104.74(4).

metrics about the iron(II) ion are essentially identical to those of **2·thf** (Table 1), with the exception of the slightly contracted Fe–Li distance of 3.021(2) Å. The Li–N contacts are also shortened significantly, in line with the smaller ionic radius of Li versus Na.

Attempts were also made to prepare homoleptic 7-azaindolide complexes of other 3d transition metals. Addition of 4 equiv of 7-azaindolide to $NiCl_2$ under identical conditions used for the synthesis of **1**–**3** afforded the previously reported paddlewheel complex, $[Ni_2(\mu\text{-AzaIn})_4]$ eq 5.[51] It therefore

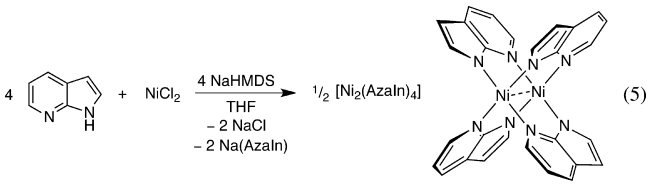

(5)

appears that in the case of nickel the presence of additional 7-azaindolide equivalents is not sufficient to suppress formation of the bimetallic species. We obtained the crystal structure of the dichloromethane solvate of the dinickel compound, which displays disordered 7-azaindolide ligands as also observed in the structure of the published dimethylformamide solvate (see Supporting Information).[51] Similar reactions were also investigated for both $CrCl_2$ and $CrCl_3$ although isolation of a monometallic Cr complex was unsuccessful.[52] During several attempts, the paddlewheel complex $[Cr_2(\mu\text{-AzaIn})_4Cl_2]^{2-}$ [53] was observed as a minor product.

Given the relative scarcity of mid-to-late transition metal complexes containing four anionic nitrogen-based ligands, we were curious as to the extent to which the azaindolide ligands engender a highly reducing environment at the metal center. The electrochemical behavior of **2** was therefore examined by cyclic voltammetry. We reasoned that **2** would exhibit the most straightforward electrochemistry of the three congeners given the multitude of tetrahedral iron(II) complexes that display a reversible $Fe^{II/III}$ couple. The cyclic voltammogram of **2** was found to be quite solvent-dependent, and acetonitrile was observed to be the best medium. This solvent dependence is most likely a result of differing solvation of the sodium cations (vide supra). In acetonitrile, **2** displays a quasi-reversible anode event at −0.73 V versus the Fc/Fc^+ couple. We assign this event to the $Fe^{II/III}$ couple (Figure 4). This low value is consistent with an electron-rich environment created by the azaindolide ligands. Similar, albeit even lower values for the $Fe^{II/III}$ couple were observed for related four-coordinate homoleptic complexes of iron containing the di-*tert*-butyl ketimide ligand.[54,55]

To gauge the ligand-field strength of the 7-azaindolide ligand, we next examined the electronic absorption spectrum of **3**. Both complexes **1** and **2** are colorless in solution and lack optical bands in the visible to near-IR region (5000–28 000 cm^{-1}). The spectrum of **3** in toluene is depicted in Figure 5. Two bands are observable between 6000 and 24 000 cm^{-1} corresponding to ligand-field transitions of $^4T_1(F) \leftarrow {}^4A_2$ and $^4T_1(P) \leftarrow {}^4A_2$ parentage. Both absorption envelopes display multiple bands possibly resulting from spin–orbit coupling and/or small distortions from perfectly tetrahedral geometry. From the average energies of these bands, a ligand-field splitting parameter (Δ_t) of 4980 cm^{-1} and a Racah parameter (B') of 697 cm^{-1} were determined for the complex (see Supporting Information). Therefore, the ligand-field strength of the κ^1-N1 azaindolide ligand appears to be close to the upper

Table 1. Selected Average Bond Distances (Å) and Angles (deg) for Complexes 1–3

metric	1·tol	2·thf	2·benz	3·thf	3·tol
$M-N_{pyr}$	2.085(2)	2.042(2)	2.041(2)	2.013(2)	2.004(2)
N–M–N	109.42(8)	109.43(8)	109.48(7)	109.43(6)	109.37(11)
M–Na	3.237(1)	3.287(1)	3.215(1)	3.316(1)	3.218(1)
$Na-N_{py}$	2.437(2)	2.384(2)	2.386(2)	2.383(2)	2.424(3)
$Na-N_{pyr}$	2.517(2)	2.539(3)	2.504(2)	2.541(2)	2.524(3)

DOI: 10.1021/acs.inorgchem.5b01732
Inorg. Chem. 2015, 54, 9637–9645

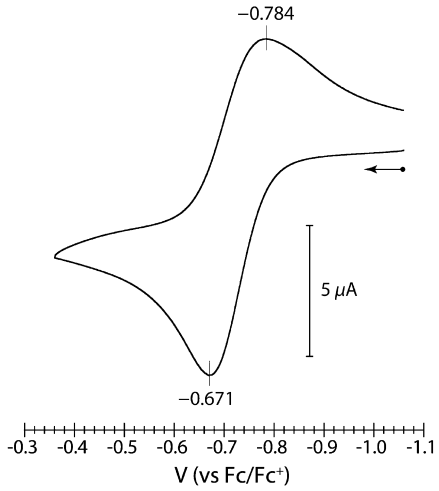

Figure 4. Cyclic voltammogram of **2·mthf** in THF at a platinum electrode. Scan rate is 50 mV/s, and the supporting electrolyte is 0.1 M Bu_4NPF_6.

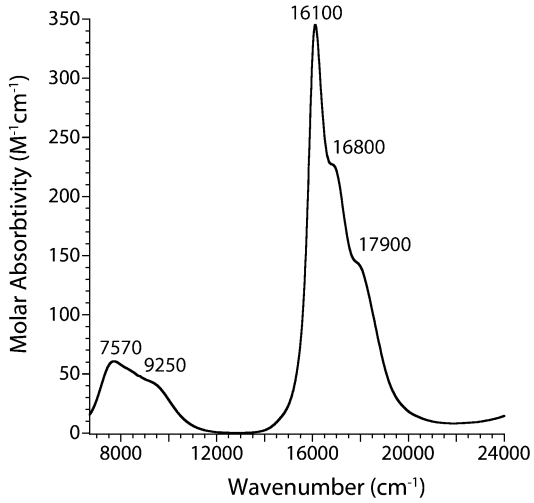

Figure 5. Region of the electronic absorption spectrum for **3** in toluene showing the ligand-field transitions. Band energies are labeled on the spectrum.

limit for known homoleptic tetrahedral complexes of Co(II).[56−61]

Synthesis of an Fe 4-Azaindolide Complex. As a means of comparing the structure and reactivity of the 7-azaindolide complexes with a different azaindole isomer, 4-azaindole was explored as a ligand to iron(II). To the best of our knowledge, only one example of a transition metal complex of 4-azaindole in any protonation state has been reported previously.[62] Accordingly, 4 equiv of 4-azaindole were reacted with $FeCl_2(THF)_{1.5}$ in THF in the presence of NaHMDS. Upon addition of the base, immediate precipitation of a yellow solid was observed (eq 6, **6·thf**). The yellow solid is insoluble in

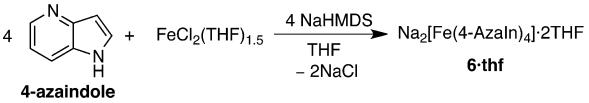

(6)

hydrocarbons and ethers, but it dissolves sparingly in acetonitrile. Combustion analysis and ^{1}H NMR spectroscopy demonstrate that 2 equiv of solvent are retained per iron center in similar fashion to **2**.

Attempts were made to crystallize **6** from acetonitrile to obtain material suitable for X-ray diffraction. Unfortunately, multiple crystallization conditions only afforded powders. Despite the lack of information concerning the solid-state structure of **6**, solution data support a structure for the complex very similar to that of **2**. ^{1}H NMR spectra of $Na_2[Fe(4\text{-}AzaIn)_4]\cdot 2L$ (L = THF or CH_3CN) in acetonitrile-d_3 display five paramagnetically shifted resonances indicating equivalency of the four 4-azaindolide ligands at room temperature. Furthermore, the cyclic voltammogram of **6** in acetonitrile displays a quasi-reversible anode event centered at −0.72 V (see Supporting Information). The position of this event is very comparable to that observed for **2** and demonstrates that **6** is most likely a homoleptic azaindolide complex of iron(II) with pyrrolide coordination.

Computational Studies. Spin-unrestricted density functional theory (DFT) calculations were utilized to better understand the bonding and electronic structure of the series of metal 7-azaindolide complexes (**1**−**3**). Geometry optimizations for **1**−**3** produced calculated structures in good agreement with crystallographic data (see Supporting Information). For each complex, the B3LYP,[63,64] BP86,[65,66] PBEPBE,[67] and M06l[68] functionals were screened to identify the functional that produced an optimized structure in closest agreement to the crystallographic data and that generated reasonable results for the molecular orbital and charge decomposition analyses (vide infra). In addition, calculations were performed on both **3·tol** and **3·thf** to confirm that differing solvation of the sodium cations does not substantially alter the electronic structure of the transition metal ions (see Supporting Information).

DFT calculations on **1**−**3** predict a high-spin (H.S.) electronic ground state in agreement with experimental magnetic susceptibilities. The electronic structure for each complex can be described by the frontier molecular orbitals, which have substantial d orbital character. The calculated energy diagram shown in Figure 6 showcases β orbital energies for all three complexes, and representative depictions of the molecular orbitals for **2** appear in Figure 7. For complex **1** there are no occupied d orbitals in the β manifold (H.S., $S = 5/2$),

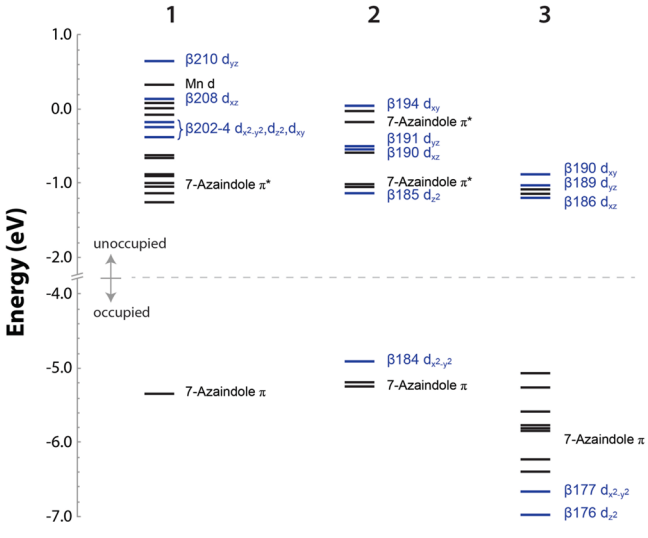

Figure 6. Computed frontier molecular orbital diagrams for complexes **1**−**3**.

DOI: 10.1021/acs.inorgchem.5b01732
Inorg. Chem. 2015, 54, 9637−9645

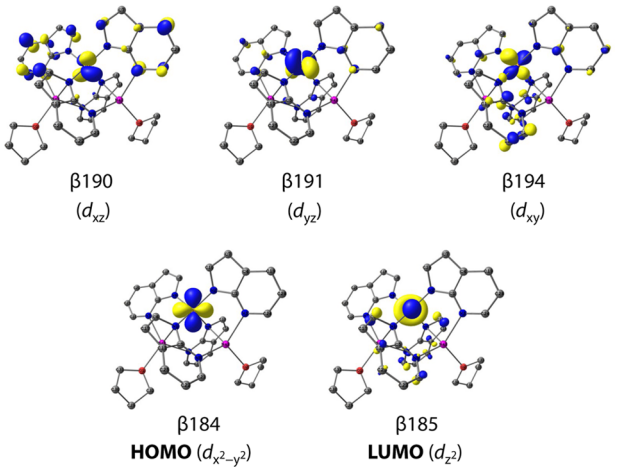

Figure 7. Selected frontier molecular orbitals for **2**·**thf**.

while for **2** (H.S., $S = 2$) and **3** (H.S., $S = 3/2$) there are one and two occupied d orbitals in the β manifold, respectively. Note that the d orbital ordering varies slightly within the series of complexes but is still consistent with a simple crystal field theory model for a tetrahedron, having the formally e set of d orbitals lower in energy than the t_2 set.

Charge decomposition and Mayer bond order analyses (CDA and MBO, respectively) were also performed for the series of 7-azaindolide complexes. The details of CDA have been given previously.[69−71] CDA allows for the magnitudes of charge donation to be calculated. In the cases of complexes **1**−**3**, charge donation can occur from the 7-azaindolide ligands to the metal center, while back-donation can occur in the opposite sense. The results of the CDA indicate that the total donation from the AzaIn ligand to the metal is the highest for **3** with 1.408 electrons, followed by **2** with 1.350 electrons, and finally **1** with 1.066 electrons (Table 2). Note that the back-donation also has a large increase going from **1** with 0.055 electrons, to **2** with 0.205 electrons, but decreases slightly for **3** with 0.194 electrons. Nevertheless, the trend holds for the total net charge donation to the metal center with the cobalt congener having the highest value of 1.214 electrons, followed by the iron and cobalt complexes with 1.145 electrons and 1.011 electrons, respectively. This observed trend likely arises from the increase in electronegativity seen going across the periodic table, allowing for more overall electron density to be transferred to the metal center. Consequently, these ligands can be regarded as nearly pure σ-donor ligands with very little π-accepting character. This description is also consistent with the relatively large Racah parameter, B', calculated for **3** (vide supra).

Mayer bond orders (MBOs) can be described as an extension of the Wiberg bond order that takes into account the ionic character of bonds and delocalization effects.[72] Note that an MBO of one occurs for a covalent single bond in a simple molecule using a small basis set. Results from the MBO analysis for complexes **1**−**3** indicate that the bonding is rather ionic across the series with an average MBO of 0.463 (Table 3).

Table 3. Mayer Bond Orders of M−N Bonds in Complexes 1−3

complex	M−N1	M−N2	M−N3	M−N4
1	0.350	0.350	0.476	0.476
2	0.415	0.416	0.533	0.531
3	0.453	0.453	0.553	0.552

Notably, the MBO analysis displays a similar trend as the CDA, with the overall bond order increasing across the periodic table. This is consistent with the finding that the Co center receives the largest amount of donation from the 7-azaindolide ligands, thereby strengthening the M−N bonds. Since covalency is generally defined as the sharing of electrons, it is not surprising to find that the Co complex has the most covalent M−N bonds with two electrons being transferred from the metal upon binding to the ligands and a total of ∼1.2 electrons being transferred back to the metal center from the ligands. It is also noteworthy that for the two 7-azaindolide ligands whose pyrrolic nitrogen atoms are involved in bonding with the sodium cations (N1 and N2), the MBOs are substantially smaller than for the two ligands that lack this interaction (N3 and N4). This fact reflects the removal of extra electron density by the sodium ion from the 7-azaindolide ligands.

CONCLUSIONS

In conclusion, we have demonstrated the synthesis of homoleptic complexes of divalent Mn, Fe, and Co containing the 7-azaindolide ligand. Each complex is tetrahedral, demonstrating exclusive κ^1-N1 coordination of the azaindolide ligand to the transition metal ion. The alkali metal counterions are tightly associated with each complex but undergo differing degrees of dissociation in polar solvents. Electronic absorption spectroscopy on the cobalt analogue along with DFT calculations on all three complexes demonstrate that 7-azaindolide is a nearly pure σ-donor ligand with a substantial degree of ionic character in its bonding to transition metals. In addition to the 7-azaindolide complexes, we have also prepared one of the first examples of a transition metal complex containing the 4-azaindolide ligand. Spectroscopic characterization of this complex demonstrates that it most likely adopts a solution structure nearly identical to that of the 7-azaindolide complexes. Future work will investigate if these azaindolide platforms can be used to generate heterometallic assemblies by substitution of the alkali metal cations with those of transition metal ions.

EXPERIMENTAL SECTION

General Comments. All manipulations were performed in a Vacuum Atmospheres glovebox under an atmosphere of purified

Table 2. Results of Charge Decomposition Analysis[a] for Complexes 1−3

complex	total donation (AzaIn→M)	total back donation (M→AzaIn)	total net charge donation
1[b]	1.066 e$^-$	0.055 e$^-$	1.011 e$^-$
2[c]	1.350 e$^-$	0.205 e$^-$	1.145 e$^-$
3[b]	1.408 e$^-$	0.194 e$^-$	1.214 e$^-$

[a]CDA includes contributions from both α and β spin manifolds. [b]Geometry optimization with the BP86 functional and energy calculations with the B3LYP functional. [c]Geometry optimization with the pbepbe functional and energy calculations with the B3LYP functional.

DOI: 10.1021/acs.inorgchem.5b01732
Inorg. Chem. 2015, 54, 9637−9645

nitrogen. Tetrahydrofuran, diethyl ether, pentane, dichloromethane, toluene, and acetonitrile were purified by sparging with argon and passage through two columns packed with 4 Å molecular sieves. Benzene, 2-methyltetrahydrofuran, and benzene-d_6 were dried over sodium ketyl and vacuum-distilled prior to use. Acetonitrile-d_3 was sparged with nitrogen and stored over 4 Å molecular sieves prior to use. ^{1}H NMR spectra were recorded at 25 °C on a Varian Inova spectrometer operating at 500 MHz (^{1}H). Chemical shift values were referenced to the residual protium resonances of the deuterated solvents. Because of the paramagnetic nature of the complexes, all ^{1}H NMR resonances appeared as singlets. Full width at half-maximum (fwhm) values are reported in hertz for selected azaindole hydrogen atoms. UV−vis−NIR spectra were recorded on a Cary-1000 spectrophotometer in airtight Teflon-capped quartz cells. Cyclic voltammetry was performed in acetonitrile at 25 °C on a CH Instruments 620D electrochemical workstation. A 3-electrode setup was employed comprising a platinum working electrode, platinum wire auxiliary electrode, and a Ag/AgCl quasi-reference electrode. Triply recrystallized Bu_4NPF_6 was used as the supporting electrolyte. All electrochemical data were referenced internally to the ferrocene/ferrocenium couple at 0.00 V. Solution magnetic susceptibility measurements were determined by the Evans method without a solvent correction using reported diamagnetic corrections.[73] Elemental analyses were performed by the CENTC Elemental Analysis Facility at the University of Rochester.

Materials. 7-Azaindole, 4-azaindole, metal hexamethyldisilazides (M = Li, K, and Na), and Kryptofix 222 (4,7,13,16,21,24-hexaoxa-1,10-diazabicyclo[8.8.8]hexacosane) were purchased from commercial suppliers and used as received. Precursor metal salts $FeCl_2(THF)_{1.5}$ and $MnCl_2(THF)_{1.6}$ were prepared by published procedures.[74,75] Anhydrous $CoCl_2$ and $NiCl_2$ was purchased from Strem Chemical Co. and used as received.

X-ray Data Collection and Structure Solution Refinement. Crystals suitable for X-ray diffraction were mounted in Paratone oil onto a glass fiber and frozen under a nitrogen cold stream maintained by an X-Stream low-temperature apparatus. The data for all structures except **5·thf** were collected at 98(2) K using a Rigaku AFC12/Saturn 724 CCD fitted with Mo Kα radiation (λ = 0.710 73 Å). Data collection and unit cell refinement were performed using Crystal Clear software.[76] Data processing and absorption correction, giving minimum and maximum transmission factors, were accomplished with Crystal Clear and ABSCOR, respectively.[76,77] The data for **5·thf** were obtained at 120(2) K using a Bruker APEX2 system fitted with Mo Kα radiation. Data collection and unit cell refinement were performed with the Bruker SAINT software.[78] All structures were solved by direct methods and refined on F^2 using full-matrix, least-squares techniques with SHELXL-97.[79,80] All non-hydrogen atoms were refined with anisotropic displacement parameters. All carbon-bound hydrogen atom positions were determined by geometry and refined by a riding model. Crystallographic data and refinement parameters can be found in the Supporting Information.

Computational Details. Spin-unrestricted DFT calculations were performed using the Gaussian 09 package.[81] Geometry optimizations of **1·tol**, **3·tol**, and **3·thf** were performed with the BP86 exchange-correlation functional[65,66] and the TZVP basis set[82] on all atoms. Geometry optimization of **2·thf** was performed using the PBEPBE exchange-correlation functional[67] and the TZVP basis set on all atoms. The geometries of all complexes were fully optimized starting from X-ray crystal structures and were found to have all real (positive) frequencies.

Further calculations of molecular orbitals (MOs) utilized the B3LYP[63,64] functional with the TZVP basis set on all atoms. Molecular orbitals obtained from the Gaussian calculations were plotted with the Chemcraft program. Atomic charges and spin densities were calculated using Mulliken population analysis (MPA). The AOMix program[83,84] was used to calculate MO compositions. The analysis of the MO compositions in terms of fragment molecular orbitals (FOs), Mayer bond orders (MBOs), total overlap populations, and charge decomposition analysis (CDA)[85,86] were performed using AOMix-FO.[83]

Na_2[Mn(AzaIn)$_4$]·2L, 1. A vial was charged with 119 mg (1.01 mmol) of 7-azaindole, 59.4 mg (254 μmol) of $MnCl_2(THF)_{1.5}$, and 5 mL of toluene. The resulting suspension was stirred for 5 min prior to addition of 188 mg (1.03 mmol) of NaHMDS. The mixture became homogeneous and was stirred for 1 h at ambient temperature during which time a precipitate (NaCl) formed. All volatiles were removed in vacuo, and the remaining residue was redissolved in THF and filtered through Celite. Evaporation of the THF afforded 163 mg (90% yield; L = THF) of the desired material as a white solid. Crystals suitable for X-ray diffraction (L = toluene) were grown by vapor diffusion of pentane into a saturated toluene solution. Analytically pure material (L = 2-MeTHF) was obtained by vapor diffusion of pentane into a saturated 2-MeTHF solution. ^{1}H NMR (C_6D_6) δ, ppm: δ 25.0 (v br s), 13.4 (br s), 9.7 (br s), 3.6 (br s, *MeTHF*), 3.4 (br s, *MeTHF*), 1.5 (br s, *MeTHF*), 1.37 (s, *MeTHF*), 1.0 (br s, *MeTHF*), −7.3 (v br). μ_{eff} (Evans, C_6D_6): 5.7(2) μ_B. Anal. Calcd for $C_{38}H_{40}MnN_8Na_2O_2$: C, 61.54; H, 5.44, 15.11. Found: C, 61.47; H, 5.39; N, 14.81%.

Na_2[Fe(AzaIn)$_4$]·2L, 2. A flask was charged with 115 mg (491 μmol) of $FeCl_2(THF)_{1.5}$, 232 mg (1.96 mmol) of 7-azaindole, and 15 mL of THF. To the resulting yellow solution was added 390 mg (1.99 mmol) of NaHMDS. The mixture was stirred for 30 min at ambient temperature, during which time it became more orange in color, and a precipitate formed. The reaction mixture was filtered through Celite to separate NaCl, and all volatiles were removed in vacuo. The remaining solid residue was triturated with pentane and collected by filtration yielding 292 mg (86%; L = THF) of a pale yellow solid. Crystals suitable for X-ray diffraction (L = benzene or THF) were grown by vapor diffusion of pentane into a saturated benzene or THF solution. Analytically pure material (L = 2-MeTHF) was obtained by vapor diffusion of pentane into a saturated 2-MeTHF solution. ^{1}H NMR (C_6D_6) δ, ppm: 31.65 (s, 55 Hz, 4H), 9.8 (br s, 600 Hz, 4H), 4.7 (br s, 960 Hz, 4H), 1.83 (s, 2H, *MeTHF*), 1.53 (s, 2H, *MeTHF*), 1.50 (s, 2H, *MeTHF*), 0.68 (s, 2H, *MeTHF*), 0.56 (s, 4H, *MeTHF*), 0.03 (s, 2H, *MeTHF*), −0.81 (s, 6H, *MeTHF*), −8.81 (s, 56 Hz, 4H). ^{1}H NMR (CD_3CN) δ, ppm: 68.4 (br s, 1200 Hz, 4H), 30.40 (s, 34 Hz, 4H), 10.40 (s, 95 Hz, 4H), 8.18 (s, 80 Hz, 4H), −7.23 (s, 27 Hz, 4H). μ_{eff} (Evans, C_6D_6): 5.0(2) μ_B. Anal. Calcd for $C_{38}H_{40}FeN_8Na_2O_2$: C, 61.46; H, 5.43; N, 15.09. Found: C, 61.44; H, 5.48; N, 15.00%.

Na_2[Co(AzaIn)$_4$]·2L, 3. A flask was charged with 157 mg (1.21 mmol) of anhydrous $CoCl_2$, 571 mg (4.83 mmol) of 7-azaindole, and 15 mL of THF. The resulting blue mixture was stirred for 5 min prior to addition of 895 mg (4.88 mmol) of NaHMDS. A deep blue solution with a white precipitate formed immediately and was allowed to stir for 1 h. The mixture was filtered through Celite to remove NaCl, and all volatiles were removed in vacuo. The remaining solid was washed with pentane and dried in vacuo to afford 697 mg (80%; L = THF) of blue microcrystals. Crystals suitable for X-ray diffraction (L = THF or toluene) were grown by vapor diffusion of pentane into a saturated THF or toluene solution. Analytically pure material (L = 2-MeTHF) was obtained by vapor diffusion of pentane into a saturated 2-MeTHF solution. ^{1}H NMR (C_6D_6) δ, ppm: 31.5 (br s, 4H), 26.7 (v br s, 4H), 12.3 (br s, 4H), 4.38 (s, 2H, *MeTHF*), 4.29 (s, 2H, *MeTHF*), 4.11 (s, 2H, *MeTHF*), 1.84 (s, 4H, *MeTHF*), 1.74 (s, 2H, *MeTHF*), 1.60 (s, 6H, *MeTHF*), 1.39 (s, 2H, *MeTHF*), −2.8 (br s, 4H). ^{1}H NMR (CD_3CN) δ, ppm: 88.6 (br s, 870 Hz, 4H), 32.02 (s, 50 Hz, 4H), 30.85 (s, 39 Hz, 4H), 10.79 (s, 75 Hz, 4H), −3.13 (s, 43 Hz, 4H). μ_{eff} (Evans, C_6D_6): 4.0(2) μ_B. Anal. Calcd for $C_{38}H_{40}N_8CoNa_2O_2$: C, 61.21; H, 5.41; N, 15.03. Found: C, 60.74; H, 5.55; N, 15.04%.

K_2[Fe(AzaIn)$_4$], 4. A vial was charged with 147 mg (1.24 mmol) of 7-azaindole, 73.1 mg (311 μmol) of $FeCl_2(THF)_{1.5}$, and 4 mL of THF. To the resulting yellow solution was added 1.38 mL (1.24 mmol) of 0.91 M KHMDS as a solution in THF. The reaction mixture was allowed to stir at ambient temperature for 1 h. All volatiles were removed in vacuo, and the remaining residue was extracted into acetonitrile and filtered through a plug of Celite. Evaporation of the acetonitrile solution and trituration with diethyl ether afforded 130 mg (69%) of the desired product as an off-white solid. Crystals suitable for X-ray diffraction were grown by vapor diffusion of pentane into a saturated solution of the complex in 4:1 benzene/THF. Analytically pure material was obtained by vapor diffusion of diethyl ether into a

DOI: 10.1021/acs.inorgchem.5b01732
Inorg. Chem. 2015, 54, 9637−9645

saturated acetonitrile solution. ^{1}H NMR (CD_3CN) δ, ppm: 70.6 (br s, 1300 Hz, 4H), 30.14 (s, 29 Hz, 4H), 13.13 (s, 85 Hz, 4H), 7.17 (s, 65 Hz, 4H), −7.04 (s, 24 Hz, 4H). μ_{eff} (Evans, CD_3CN): 5.3(2) μ_B. Anal. Calcd for $C_{28}H_{20}FeK_2N_8$: C, 55.81; H, 3.35; N, 18.60. Found: C, 55.76; H, 3.44; N, 18.61%.

Li_2[Fe(AzaIn)$_4$]·2L, 5. A vial was charged with 164 mg (1.39 mmol) of 7-azaindole and 4 mL of THF then chilled to −196 °C. To the stirring, thawing solution was added 232 mg (1.39 mmol) of LiHMDS. The mixture was allowed to stir and warm to ambient temperature until homogeneous. The homogeneous solution was again chilled to −196 °C at which point 81.6 mg (347 μmol) of $FeCl_2(THF)_{1.5}$ was added. The thawing reaction mixture was allowed to stir at ambient temperature, during which time it acquired a peach color, and an off-white precipitate formed. After it stirred for 2 h at ambient temperature the reaction mixture was chilled to −30 °C to encourage further precipitation of the off-white solid. The precipitate was isolated by filtration, washed with pentane, and dried in vacuo to afford 197 mg (83%, L = THF) of a white solid. Analytically pure material was obtained by vapor diffusion of pentane into a saturated benzene solution. Crystals suitable for X-ray diffraction were grown in similar fashion. Material purified in this way was found to retain both equivalents of THF and an additional equivalent of benzene. ^{1}H NMR (C_6D_6) δ, ppm: 71.1 (br s, 2H), 59.8 (br s, 2H), 31.17 (s, 2H), 29.00 (s, 2H), 13.1 (br s, 2H), 6.4 (br s, 2H), 5.3 (br s, 2H), 4.0 (br s, 2H), −0.04 (m, 16H, *THF*), −7.21 (s, 4H). ^{1}H NMR (CD_3CN) δ, ppm: 64.0 (v br s, 4H), 29.63 (s, 75 Hz, 4H), 9.1 (br s, 640 Hz, 4H), 5.8 (br s, 420 Hz, 4H), −6.90 (s, 42 Hz, 4H). μ_{eff} (Evans, CD_3CN): 5.1(2) μ_B. Anal. Calcd for $C_{36}H_{36}FeLi_2N_8O_2 \cdot C_6H_6$: C, 66.33; H, 5.57; N, 14.73. Found: C, 66.53; H, 5.89; N, 14.50%.

Na_2[Fe(4-AzaIn)$_4$]·2L, 6. A round-bottom flask was charged with 200 mg (851 μmol) of $FeCl_2(THF)_{1.5}$ and 402 mg (3.40 mmol) of 4-azaindole. The solids were dissolved in 10 mL of THF giving rise to a yellow solution. To the solution was added 624 mg (3.40 mmol) of NaHMDS at which point a yellow precipitate immediately formed. The reaction mixture was allowed to stir for an additional 15 min before the precipitate was isolated by filtration. The yellow solid was washed generously with pentane then dried under vacuum to afford 799.4 mg of a material containing the desired complex (L = THF), NaCl, and THF. Small (∼20 mg) quantities of analytically pure material (L = CH_3CN) were obtained by vapor diffusion of ether into saturated acetonitrile solutions. Attempts to grow crystals of the complex suitable for X-ray diffraction were unsuccessful. ^{1}H NMR (CD_3CN) δ, ppm: 73.7 (br s, 860 Hz, 4H), 11.26 (s, 92 Hz, 4H), 3.81 (s, 43 Hz, 4H), −3.24 (s, 37 Hz, 4H), −15.9 (br s, 680 Hz, 4H). Anal. Calcd for $C_{32}H_{26}FeN_{10}Na_2$: C, 58.91; H, 4.02; N, 21.47. Found: C, 59.10; H, 4.24; N, 20.76%.

■ ASSOCIATED CONTENT

Supporting Information

The Supporting Information is available free of charge on the ACS Publications website at DOI: 10.1021/acs.inorgchem.5b01732.

Additional NMR spectra of compounds **1**−**6**; cyclic voltammogram of **6·acn**; solid-state renderings of **1·mTHF**, **2·THF**, **3·tol**, **2·benz**, **4**, and [$Ni_2(\mu$-AzaIn)$_4$]; computational data for compounds **1**−**3**. (PDF)

Crystallographic information. (CIF)

■ AUTHOR INFORMATION

Corresponding Author

*E-mail: zachary.tonzetich@utsa.edu.

Author Contributions

§These authors contributed equally.

The manuscript was written through contributions of all authors. All authors have given approval to the final version of the manuscript.

Notes

The authors declare no competing financial interest.

■ ACKNOWLEDGMENTS

This paper is dedicated to Professor Judith A. Walmsley. The authors acknowledge the Welch Foundation (AX-1772 to Z.J.T.) for financial support of this work. M.L.K. is partially funded by the NIH (MARC GM007717). The CENTC Elemental Analysis Facility is supported by NSF (CHE-0650456). The authors thank Prof. L. Do for assistance with crystallographic measurements.

■ REFERENCES

(1) Yakhontov, L. N.; Prokopov, A. A. *Russ. Chem. Rev.* **1980**, *49*, 428.

(2) Mérour, J.-Y.; Joseph, B. *Curr. Org. Chem.* **2001**, *5*, 471−506.

(3) Popowycz, F.; Routier, S.; Joseph, B.; Mérour, J.-Y. *Tetrahedron* **2007**, *63*, 1031−1064.

(4) Hogan, M.; Cotter, J.; Claffey, J.; Gleeson, B.; Wallis, D.; O'Shea, D.; Tacke, M. *Helv. Chim. Acta* **2008**, *91*, 1787−1797.

(5) Przyojski, J. A.; Myers, N. N.; Arman, H. D.; Prosvirin, A.; Dunbar, K. R.; Natarajan, M.; Krishnan, M.; Mohan, S.; Walmsley, J. A. *J. Inorg. Biochem.* **2013**, *127*, 175−181.

(6) Dominguez-Martin, A.; Choquesillo-Lazarte, D.; Dobado, J. A.; Vidal, I.; Lezama, L.; Gonzalez-Perez, J. M.; Castineiras, A.; Niclos-Gutierrez, J. *Dalton Trans.* **2013**, *42*, 6119−6130.

(7) Domínguez-Martín, A.; Brandi-Blanco, M. d. P.; Matilla-Hernández, A.; Bakkali, H. E.; Nurchi, V. M.; González-Pérez, J. M.; Castiñeiras, A.; Niclós-Gutiérrez, J. *Coord. Chem. Rev.* **2013**, *257*, 2814−2838.

(8) Xu, X.; Yi, J.; Jing, Z. *Acta Poly. Sinica (Gaofenzi Xuebao)* **2001**, 683−686.

(9) Cotton, F. A.; Lay, D. G.; Millar, M. *Inorg. Chem.* **1978**, *17*, 186−188.

(10) Oro, L. A.; Ciriano, M. A.; Villarroya, B. E.; Tiripicchio, A.; Lahoz, F. J. *J. Chem. Soc., Dalton Trans.* **1985**, 1891−1898.

(11) Cabeza, J. A.; Oro, L. A.; Tiripicchio, A.; Tiripicchio-Camellini, M. *J. Chem. Soc., Dalton Trans.* **1988**, 1437−1444.

(12) Allaire, F.; Beauchamp, A. L. *Inorg. Chim. Acta* **1989**, *156*, 241−249.

(13) Dufour, P.; Dartiguenave, Y.; Dartiguenave, M.; Dufour, N.; Lebuis, A.-M.; Bélanger-Gariépy, F.; Beauchamp, A. L. *Can. J. Chem.* **1990**, *68*, 193−201.

(14) Poitras, J.; Beauchamp, A. L. *Can. J. Chem.* **1994**, *72*, 2339−2347.

(15) Sánchez, G.; Ruiz, F.; Garcia, J.; Carmen de Arellano, M. R.; López, G. *Helv. Chim. Acta* **1997**, *80*, 2477−2485.

(16) Kong, F.-S.; Wong, W.-T. *J. Chem. Soc., Dalton Trans.* **1997**, 1237−1242.

(17) Tayebani, M.; Feghali, K.; Gambarotta, S.; Yap, G. P. A.; Thompson, L. K. *Angew. Chem., Int. Ed.* **1999**, *38*, 3659−3661.

(18) Cotton, F. A.; Felthouse, T. R. *Inorg. Chem.* **1981**, *20*, 600−608.

(19) Sheldrick, W. S. *Z. Naturforsch., B: J. Chem. Sci.* **1982**, *37*, 653.

(20) Poitras, J.; Beauchamp, A. L. *Can. J. Chem.* **1992**, *70*, 2846−2855.

(21) Lebuis, A.-M.; Beauchamp, A. L. *Can. J. Chem.* **1993**, *71*, 2060−2069.

(22) Poitras, J.; Beauchamp, A. L. *Can. J. Chem.* **1994**, *72*, 1675−1683.

(23) Choquesillo-Lazarte, D.; Domínguez-Martín, A.; Matilla-Hernández, A.; Sánchez de Medina-Revilla, C.; González-Pérez, J. M.; Castiñeiras, A.; Niclós-Gutiérrez, J. *Polyhedron* **2010**, *29*, 170−177.

(24) Wu, Q.; Lavigne, J. A.; Tao, Y.; D'Iorio, M.; Wang, S. *Inorg. Chem.* **2000**, *39*, 5248−5254.

(25) Bland, B. R. A.; Gilfoy, H. J.; Vamvounis, G.; Robertson, K. N.; Cameron, T. S.; Aquino, M. A. S. *Inorg. Chim. Acta* **2005**, *358*, 3927−3936.

DOI: 10.1021/acs.inorgchem.5b01732
Inorg. Chem. 2015, 54, 9637−9645

(26) Štarha, P.; Marek, J.; Trávníček, Z. *Polyhedron* **2012**, *33*, 404−409.
(27) Kosaka, W.; Yamamoto, N.; Miyasaka, H. *Inorg. Chem.* **2013**, *52*, 9908−9914.
(28) Switlicka-Olszewska, A.; Machura, B.; Mrozinski, J.; Kalinska, B.; Kruszynski, R.; Penkala, M. *New J. Chem.* **2014**, *38*, 1611−1626.
(29) Chan, C.-K.; Guo, C.-X.; Cheung, K.-K.; Li, D.; Che, C.-M. *J. Chem. Soc., Dalton Trans.* **1994**, 3677−3682.
(30) Wagler, J.; Hill, A. F. *Organometallics* **2008**, *27*, 2350−2353.
(31) Ruiz, J.; Rodriguez, V.; de Haro, C.; Espinosa, A.; Perez, J.; Janiak, C. *Dalton Trans.* **2010**, *39*, 3290−3301.
(32) Ashenhurst, J.; Wu, G.; Wang, S. *J. Am. Chem. Soc.* **2000**, *122*, 2541−2547.
(33) Wang, S. *Coord. Chem. Rev.* **2001**, *215*, 79−98.
(34) Zhao, S.-B.; Wang, S. *Chem. Soc. Rev.* **2010**, *39*, 3142−3156.
(35) Liu, S.-F.; Wu, Q.; Schmider, H. L.; Aziz, H.; Hu, N.-X.; Popović, Z.; Wang, S. *J. Am. Chem. Soc.* **2000**, *122*, 3671−3678.
(36) Song, D.; Jia, W. L.; Wu, G.; Wang, S. *Dalton Trans.* **2005**, 433−438.
(37) Wahlicht, S.; Brendler, E.; Heine, T.; Zhechkov, L.; Wagler, J. *Organometallics* **2014**, *33*, 2479−2488.
(38) Song, D.; Wang, S. *Organometallics* **2003**, *22*, 2187−2189.
(39) Tsoureas, N.; Owen, G. R.; Hamilton, A.; Orpen, A. G. *Dalton Trans.* **2008**, 6039−6044.
(40) Tsoureas, N.; Bevis, T.; Butts, C. P.; Hamilton, A.; Owen, G. R. *Organometallics* **2009**, *28*, 5222−5232.
(41) Tsoureas, N.; Haddow, M. F.; Hamilton, A.; Owen, G. R. *Chem. Commun.* **2009**, 2538−2540.
(42) Tsoureas, N.; Nunn, J.; Bevis, T.; Haddow, M. F.; Hamilton, A.; Owen, G. R. *Dalton Trans.* **2011**, *40*, 951−958.
(43) Bazhenova, T. A.; Lobkovskaya, R. M.; Shibaeva, R. P.; Shilova, A. K.; Gruselle, M.; Leny, G.; Deschamps, E. *J. Organomet. Chem.* **1983**, *244*, 375−382.
(44) Buzzeo, M. C.; Iqbal, A. H.; Long, C. M.; Millar, D.; Patel, S.; Pellow, M. A.; Saddoughi, S. A.; Smenton, A. L.; Turner, J. F. C.; Wadhawan, J. D.; Compton, R. G.; Golen, J. A.; Rheingold, A. L.; Doerrer, L. H. *Inorg. Chem.* **2004**, *43*, 7709−7725.
(45) Zheng, B. N.; Miranda, M. O.; Di Pasquale, A. G.; Golen, J. A.; Rheingold, A. L.; Doerrer, L. H. *Inorg. Chem.* **2009**, *48*, 4274−4276.
(46) Cantalupo, S. A.; Lum, J. S.; Buzzeo, M. C.; Moore, C.; Di Pasquale, A. G.; Rheingold, A. L.; Doerrer, L. H. *Dalton Trans.* **2010**, *39*, 374−383.
(47) Cantalupo, S. A.; Fiedler, S. R.; Shores, M. P.; Rheingold, A. L.; Doerrer, L. H. *Angew. Chem., Int. Ed.* **2012**, *51*, 1000−1005.
(48) Marshak, M. P.; Nocera, D. G. *Inorg. Chem.* **2013**, *52*, 1173−1175.
(49) Chambers, M. B.; Groysman, S.; Villagran, D.; Nocera, D. G. *Inorg. Chem.* **2013**, *52*, 3159−3169.
(50) Tahsini, L.; Specht, S. E.; Lum, J. S.; Nelson, J. J. M.; Long, A. F.; Golen, J. A.; Rheingold, A. L.; Doerrer, L. H. *Inorg. Chem.* **2013**, *52*, 14050−14063.
(51) Peng, S.-M.; Lai, C.-H. *J. Chin. Chem. Soc.* **1988**, *35*, 325−336.
(52) Edema, J. J. H.; Gambarotta, S.; Meetsma, A.; Van Bolhuis, F.; Spek, A. L.; Smeets, W. J. J. *Inorg. Chem.* **1990**, *29*, 2147−2153.
(53) Cotton, F. A.; Murillo, C. A.; Zhou, H.-C. *Inorg. Chem.* **2000**, *39*, 3728−3730.
(54) Lewis, R. A.; Morochnik, S.; Chapovetsky, A.; Wu, G.; Hayton, T. W. *Angew. Chem., Int. Ed.* **2012**, *51*, 12772−12775.
(55) Lewis, R. A.; Wu, G.; Hayton, T. W. *J. Am. Chem. Soc.* **2010**, *132*, 12814−12816.
(56) Goodgame, D. M. L.; Goodgame, M.; Cotton, F. A. *Inorg. Chem.* **1962**, *1*, 239−245.
(57) Cotton, F. A.; Faut, O. D.; Mague, J. T. *Inorg. Chem.* **1964**, *3*, 17−21.
(58) Cotton, F. A.; Goodgame, M. *J. Am. Chem. Soc.* **1961**, *83*, 1777−1780.
(59) Cotton, F. A.; Goodgame, D. M. L.; Goodgame, M.; Sacco, A. *J. Am. Chem. Soc.* **1961**, *83*, 4157−4161.
(60) Cotton, F. A.; Goodgame, D. M. L.; Goodgame, M. *J. Am. Chem. Soc.* **1961**, *83*, 4690−4699.
(61) Zadrozny, J. M.; Telser, J.; Long, J. R. *Polyhedron* **2013**, *64*, 209−217.
(62) Sa, D. S.; Fernandes, A. F.; Silva, C. D. S.; Costa, P. P. C.; Fonteles, M. C.; Nascimento, N. R. F.; Lopes, L. G. F.; Sousa, E. H. S. *Dalton Trans.* **2015**, *44*, 13633−13640.
(63) Becke, A. D. *J. Chem. Phys.* **1993**, *98*, 1372−1377.
(64) Lee, C.; Yang, W.; Parr, R. G. *Phys. Rev. B: Condens. Matter Mater. Phys.* **1988**, *37*, 785−789.
(65) Becke, A. D. *Phys. Rev. A: At., Mol., Opt. Phys.* **1988**, *38*, 3098−3100.
(66) Perdew, J. P. *Phys. Rev. B: Condens. Matter Mater. Phys.* **1986**, *33*, 8822−8824.
(67) Perdew, J. P.; Burke, K.; Ernzerhof, M. *Phys. Rev. Lett.* **1996**, *77*, 3865−3868.
(68) Zhao, Y.; Truhlar, D. G. *J. Chem. Phys.* **2006**, *125*, 194101.
(69) Gorelsky, S. I.; Basumallick, L.; Vura-Weis, J.; Sarangi, R.; Hodgson, K. O.; Hedman, B.; Fujisawa, K.; Solomon, E. I. *Inorg. Chem.* **2005**, *44*, 4947−4960.
(70) Gorelsky, S.; Solomon, E. *Theor. Chem. Acc.* **2008**, *119*, 57−65.
(71) Fillman, K. L.; Przyojski, J. A.; Al-Afyouni, M. H.; Tonzetich, Z. J.; Neidig, M. L. *Chem. Sci.* **2015**, *6*, 1178−1188.
(72) Bridgeman, A. J.; Cavigliasso, G.; Ireland, L. R.; Rothery, J. *J. Chem. Soc., Dalton Trans.* **2001**, 2095−2108.
(73) Bain, G. A.; Berry, J. F. *J. Chem. Educ.* **2008**, *85*, 532−536.
(74) Zhao, H.; Clérac, R.; Sun, J. S.; Ouyang, X.; Clemente-Juan, J. M.; Gómez-García, C. J.; Coronado, E.; Dunbar, K. R. *J. Solid State Chem.* **2001**, *159*, 281−292.
(75) Fowles, G. W. A.; Rice, D. A.; Walton, R. A. *J. Inorg. Nucl. Chem.* **1969**, *31*, 3119−3131.
(76) *Crystal Clear;* Rigaku/MSC Inc; Rigaku Corporation: The Woodlands, TX, 2005.
(77) *ABSCOR;* Rigaku Corporation: Tokyo, Japan, 1995.
(78) Bruker. *SAINT;* Bruker AXS, Inc: Madison, WI, 2007.
(79) *SHELXTL97: Program for Refinement of Crystal Structures;* Sheldrick, G. M., University of Göttingen: Germany, 1997.
(80) Sheldrick, G. M. *Acta Crystallogr., Sect. A: Found. Crystallogr.* **2008**, *A64*, 112−122.
(81) Frisch, M. J.; Trucks, G. W.; Schlegel, H. B.; Scuseria, G. E.; Robb, M. A.; Cheeseman, J. R.; Scalmani, G.; Barone, V.; Mennucci, B.; Petersson, G. A.; Nakatsuji, H.; Caricato, M.; Li, X.; Hratchian, H. P.; Izmaylov, A. F.; Bloino, J.; Zheng, G.; Sonnenberg, J. L.; Hada, M.; Ehara, M.; Toyota, K.; Fukuda, R.; Hasegawa, J.; Ishida, M.; Nakajima, T.; Honda, Y.; Kitao, O.; Nakai, H.; Vreven, T.; Montgomery Jr., J. A.; Peralta, J. E.; Ogliaro, F.; Bearpark, M. J.; Heyd, J.; Brothers, E. N.; Kudin, K. N.; Staroverov, V. N.; Kobayashi, R.; Normand, J.; Raghavachari, K.; Rendell, A. P.; Burant, J. C.; Iyengar, S. S.; Tomasi, J.; Cossi, M.; Rega, N.; Millam, N. J.; Klene, M.; Knox, J. E.; Cross, J. B.; Bakken, V.; Adamo, C.; Jaramillo, J.; Gomperts, R.; Stratmann, R. E.; Yazyev, O.; Austin, A. J.; Cammi, R.; Pomelli, C.; Ochterski, J. W.; Martin, R. L.; Morokuma, K.; Zakrzewski, V. G.; Voth, G. A.; Salvador, P.; Dannenberg, J. J.; Dapprich, S.; Daniels, A. D.; Farkas, Ö.; Foresman, J. B.; Ortiz, J. V.; Cioslowski, J.; Fox, D. J. *Gaussian 09;* Gaussian, Inc: Wallingford, CT, 2009.
(82) Schäfer, A.; Huber, C.; Ahlrichs, R. *J. Chem. Phys.* **1994**, *100*, 5829−5835.
(83) Gorelsky, S. I. *AOMix: Program for Molecular Orbital Analysis*; http://www.sg-chem.net/, 2014.
(84) Gorelsky, S. I.; Lever, A. B. P. *J. Organomet. Chem.* **2001**, *635*, 187−196.
(85) Dapprich, S.; Frenking, G. *J. Phys. Chem.* **1995**, *99*, 9352−9362.
(86) Gorelsky, S. I.; Ghosh, S.; Solomon, E. I. *J. Am. Chem. Soc.* **2006**, *128*, 278−290.

DOI: 10.1021/acs.inorgchem.5b01732
Inorg. Chem. 2015, 54, 9637−9645